Geomechanics and Engineering, *Vol. 18, No. 1 (2019) 29-39*
DOI: https://doi.org/10.12989/gae.2019.18.1.029

Determination of the bearing capacity of model ring footings: Experimental and numerical investigations

Yakup Turedi[1a], Buse Emirler[2a], Murat Ornek[*1] and Abdulazim Yildiz[3b]

[1]Department of Civil Engineering, Iskenderun Technical University, Hatay 31200, Turkey
[2]Department of Civil Engineering, Cukurova University, Adana 01950, Turkey
[3]Department of Civil Engineering, Cukurova University, Adana 01330, Turkey

(Received September 20, 2018, Revised April 2, 2019, Accepted April 16, 2019)

Abstract. In this paper, it was presented an investigation on the load-settlement and vertical stress analysis of the ring footings on the loose sand bed by conducting both laboratory model tests and numerical analyses. A total of twenty tests were conducted in geotechnical laboratory and numerical analyses of the test models were carried out using the finite element package Plaxis 3D to find the ultimate capacities of the ring footings. Moreover, the results obtained from both foregoing methods were compared with theoretical results given in the literature. The effects of the ring width on bearing capacity of the footings and vertical stresses along the depth were investigated. Consequently, the experimental observations are in a very good agreement with the numerical and theoretical results. The variation in the bearing capacity is little when $r_i/R_o<0.3$. That means, when the ring width ratio, r_i/R_o, is equal to 0.3, this option can provide more economic solutions in the applications of the ring footings. Since, this corresponds to less concrete consumption in the ring footing design.

Keywords: model test; numerical analysis; bearing capacity; vertical stress; ring foundation; loose sand

1. Introduction

Ring footings are special types of shallow foundations. In recent years, they have been commonly used in order to support loads of the axisymmetric structures (e.g., cooling towers, water tower structures, smoke-stacks, transmission towers, radar stations, TV antennae, bridge piers, chimneys, storage tanks and silos) in engineering practice. In comparison with circular footings, ring footings are more suitable and economical because the use of the ring footings decreases the amount of the material used. Prediction of the bearing capacity, settlement and stress analyses of strip, square, rectangular and circular footings have been extensively studied for many decades. However, contrary to other geometrical shapes of the footings, fewer studies have been made related to the ring footings in the literature.

Boushehrian and Hataf (2003) investigated the bearing capacity of circular and ring footings on reinforced sand by conducting laboratory model tests along with numerical analyses. According to experimental and numerical studies, when a single layer of reinforcement was placed to optimum reinforcement embedment depth, the maximum bearing capacity was reached. They have found that maximum Bearing Capacity Ratio (BCR) is obtained from n=0.40 for the ring foundations in the numerical analyses where n is the ratio of inner diameter to outer diameter of the ring footing.

*Corresponding author, Associate Professor
E-mail: murat.ornek@iste.edu.tr
[a]Ph.D. Candidate
[b]Professor

The ultimate bearing capacity of the ring foundations supported by a sand bed with and without geogrid reinforcement was evaluated by Laman and Yildiz (2007) including numerical predictions. Consequently, the experimental observations were very compatible with the numerical predictions and also optimum BCR value was obtained from r/R=0.3 for both experimental and the numerical studies. Some numerical analyses were conducted by Moayed *et al.* (2012) to investigate the bearing capacity of the ring footings on two-layered soil. The effects of the clay layer thickness and the ratio of internal radius of the ring to external radius of the ring (r_i/r_o) were analyzed. As a consequence, the bearing capacity decreases with the increase of the value of (r_i/r_o). Experimental and numerical studies were carried out by Naderi and Hataf (2014) to investigate the bearing capacity of closely located ring and circular footings on reinforced sand. At the end of these studies, it was observed that the ultimate bearing capacity of two closely spaced circular and ring footings was maximum when they stand exactly beside each other. Benmebarek *et al.* (2012) evaluated the soil bearing capacity factor N'_γ for both smooth and rough ring footings for low and high friction associated and nonassociated Mohr-Coulomb soils using numerical computations (FLAC code). As a result, the soil bearing capacity factor N'_γ decreases with an increase in the ratio of internal radius to external radius of the ring. A series of finite element analyses were evaluated by Choobbasti *et al.* (2010) to investigate the bearing capacity and settlement of smooth and rough ring footing. In these analyses, the results of the geotechnical studies of Kazeroon cooling tower were used as input parameters. The analyses have showed that the bearing capacity of rough ring footing is obviously

http://www.techno-press.org/?journal=gae&subpage=7
ISSN: 2005-307X (Print), 2092-6219 (Online)

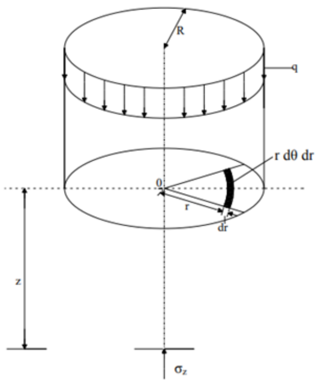

Fig. 1 Vertical stress under uniformly loaded circular footing

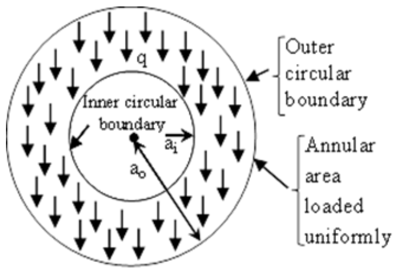

Fig. 2 Uniformly loaded annular area (ring footing)

higher than that of the smooth footing. When considering the stresses in the soil medium, it has been seen that soil's own weight and applied the external loads to the soil create stresses within the soil mass. This stress varies depending on the severity of the applied load, the soil properties and the dimensions of the area where the load is applied. Since the soils are very complex materials, making exactly stress-deformation analysis is very difficult in the soil. Therefore, theory of elasticity which is an approximate solution for the soil behavior is often used. In the literature, the most of researchers investigating the soil stress behavior on circular, square, strip, etc. have been used the rules of the theory of elasticity. Yodsa-nga *et al.* (2012) investigated stress distribution in loose sand under surcharge loading and spread footing with field testing and numerical modelling. The stresses were predicted using three numerical methods (Boussinesq's, Walter's and a linear finite element model). Consequently, it was suggested that the numerical methods allowed more realistic estimation for the contact pressure pattern. A method, called the method of images, was suggested by Hazzard *et al.* (2007). This method allows for accurate calculation of stresses in layered materials where large stiffness differences exist between layers. Shortly, the tests were conducted to compare the stress results obtained from the method of images with the results obtained from the Boussinesq method and three-dimensional finite element models. Consequently, this method is more accurate than the Boussinesq method and much simpler than the finite element method. Bhaskar *et al.* (2015) studied the contact stress distribution experimentally and analytically without any depth of embedment. In addition, finite element analyses with Plaxis 3D were carried out by placing footing at different depth in soil models. As a result, the contact stress distribution and settlement variation with the increase of the embedment vary depending on the soil. Hanna and Soliman-Saad (2001) were used the stress transducers to measure the horizontal and the vertical stresses. And also, they presented the results of an experimental investigation on the effect of the compaction duration in a prototype model. Keshavarz and Kumar (2017) investigated the bearing capacity of smooth and rough ring foundations by using the stress characteristics method (SCM). Sargazi and Hosseininia (2017) studied the bearing capacity of eccentrically-loaded rough ring footings placed over cohesionless soil. For this purpose, a series of 3D numerical simulations were performed by using the finite difference method. In order to consider the effect of load eccentricity, reduction factor method was applied. Comparison between the results of the numerical simulations with those of analytical solutions and experimental data has indicated a good agreement. Khatri *et al.* (2017) studied the pressure-settlement behavior of square and rectangular skirted footing on sand experimentally. The footing was subjected to a vertical load and the relative density of sand was 30%, 50%, 70%, and 87%, respectively. Also, the depth of skirt was varied from 0.25B to 1.0B. The skirted footings were found more effective for sand at relative density of 30% and 50% than at relative density of 70% and 87%. Moreover, the bearing capacity was found to increase linearly with and without skirts. Anil *et al.* (2017) investigated bearing capacities and settlement profiles of six irregularly shaped footings under the axial loading on sand numerically. The main variable considered in this study was the geometry of the footing. The three-dimensional finite element analyses of the tests were conducted with Plaxis 3D software. The finite element model results were in acceptable agreement with the results obtained from the experimental investigation. It was observed that the geometric properties of the footings significantly affected the variation of the bearing capacities and settlement profiles.

There are also researchers studying the stress distributions and the bearing capacity as experimental, numerical and theoretical approaches for different shapes of the footing (Lee *et al.* 2016, El Sawwaf and Nazir 2012, Ornek *et al.* 2012, Demir *et al.* 2014, Azmoodeh and Arafati 2015, Davarci *et al.* 2014, Kaya and Ornek 2013).

There are several theoretical and practical techniques to compute the stress in engineering applications. For the soil medium, commonly used techniques are the Boussinesq (1885) method and the Westergaard (1938) method. The Boussinesq method is probably the most popular. Boussinesq's equation can be used to calculate the vertical stresses occurring beneath the uniformly loaded circular area with a radius of R as shown in Fig. 1. Eq. (1) is the expression obtained by Boussinesq for computing vertical stress $\Delta\sigma_z$ at point P due to uniformly distributed load.

$$\Delta\sigma_z = q\left[1 - \frac{1}{\left[\left(R+z\right)^2+1\right]^{3/2}}\right] \tag{1}$$

where z is the depth and R is the radius of the circular footing.

For the ring footings, an annular area (inner radius a_i

and outer radius a_o) loaded uniformly q at a per unit area is given in Fig. 2 (Venkataramaiah 2006).

The vertical stress at the depth z beneath center of the ring footing, σ_z is given in Eq. (2).

$$\sigma_z = q\left[\frac{1}{\left\{1+\left(\frac{a_i}{z}\right)^2\right\}^{3/2}} - \frac{1}{\left\{1+\left(\frac{a_o}{z}\right)^2\right\}^{3/2}}\right] \tag{2}$$

$$\sigma_z = qK_{B_C} \tag{3}$$

where,

$$K_{B_C} = \left[\frac{1}{\left\{1+\left(\frac{a_i}{z}\right)^2\right\}^{3/2}} - \frac{1}{\left\{1+\left(\frac{a_o}{z}\right)^2\right\}^{3/2}}\right] \tag{4}$$

Similarly, it can be used in Westergaard's equation as shown below.

$$K_{B_C} = \left[\frac{1}{\sqrt{1+\left(\frac{a_i}{\eta z}\right)^2}} - \frac{1}{\sqrt{1+\left(\frac{a_o}{\eta z}\right)^2}}\right] \tag{5}$$

$$\eta = \sqrt{\frac{1-2v}{2-2v}} \tag{6}$$

where, v is the Poisson's ratio.

The main objective of this study is to investigate the stress, the bearing capacity and the settlement behavior of the ring footings on the loose sand using a small-scale laboratory model test and finite element program Plaxis 3D. And also, the results obtained from both methods have been compared with the theoretical results. A circular model footing and four different ring model footings with 0.01 m thick and 0.2 m outer diameter have been used in the model tests. The experimental and numerical approaches have indicated that the bearing capacity of the ring footings depends directly on the ratio of the inside diameter to that of outside. It is expected that the information presented in the study will provide a contribution to the literature and will be an alternative source for the design and applications of the ring footings for the geotechnical engineers.

2. Test equipment and materials

Fig. 3 shows the geometry and loading system of the model tests used in the investigation. The loadings have been conducted for two different shapes (circular and ring) and five different sizes (r_i/R_o=0.0, 0.3, 0.4, 0.5 and 0.6) of the model footings. All of the model tests have been carried out in the loose sand conditions.

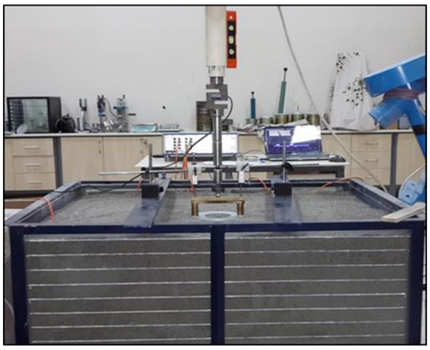

Fig. 3 Test set-up: overview

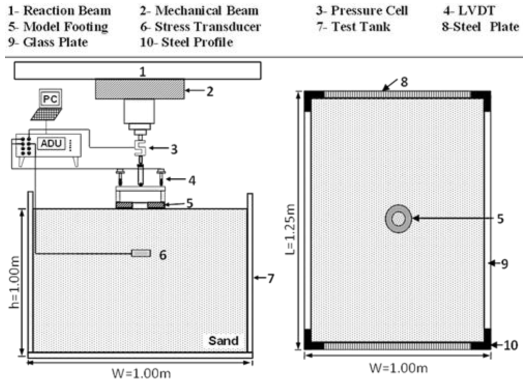

Fig. 4 Schematic figure of the experimental apparatus

The experimental program was performed in the facility of Geotechnical Laboratory of the Civil Engineering Department of Iskenderun Technical University, Turkey. The facility of Geotechnical Laboratory and a typical model are shown in Figs. 3-4.

2.1 Test tank

The model tests were conducted in a test tank with dimensions of 1.25 m×1.0 m in plan and 1.0 m in depth. The bottom and vertical edges of the tank were stiffened by using the steel profile to avoid lateral deformations during the soil placement and the loading of the model footing. While two sides of the tank consist of 10 mm-thick glass plates, the other sides consist of 3 mm steel plate and also four corners of the tank are supported with four steel columns.

In the literature, it is suggested that test tank's dimensions are at least five times longer than the diameter of the footing in order to prevent the boundary effects (Turedi and Ornek 2016).

The loading system consists of an electrically operated mechanical jack and the vertical load is applied to the model footing with a loading frame located above the tank. Stress, load and displacement measurements are taken by using a transducer, a load cell and two LVDT's with an accuracy of 0.001 mm installed between the jack and the model footing.

2.2 Model footing

The loading tests have been carried out for five rigid

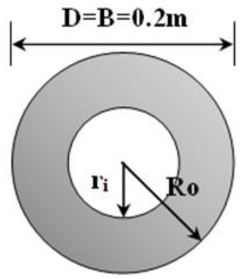

Fig. 5 Schematic view of the ring footing

Table 1 The geometries of the footings used in the tests

r_i (m)	R_o (m)	r_i (m)	R_o (m)	r_i (m)	R_o (m)	r_i (m)	R_o (m)	r_i (m)	R_o (m)
0.00	0.10	0.03	0.10	0.04	0.10	0.05	0.10	0.06	0.10
r_i/R_o 0.0		r_i/R_o 0.3		r_i/R_o 0.4		r_i/R_o 0.5		r_i/R_o 0.6	

Table 2 Properties of the sand

Property	Value
Coarse sand fraction (%)	0.00
Medium sand fraction (%)	65.00
Fine sand fraction (%)	35.00
D_{10} (mm)	0.18
D_{30} (mm)	0.28
D_{60} (mm)	0.58
Uniformity coefficient, C_u	4.46
Coefficient of curvature, C_c	1.04
Specific gravity	2.75
Dry unit weight during model tests (kN/m^3)	15.44
Cohesion, c (kN/m^2)	0.00
Classification (USCS)	SP

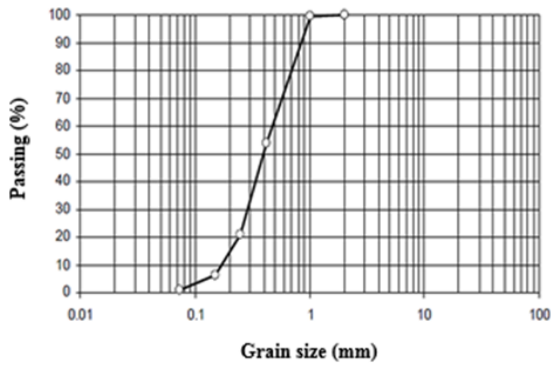

Fig. 6 Particle size distribution curve of the sand

model footings produced from the mild steel. All model footings have the thickness of 0.01 m and outer diameters of 0.20 m. The first one of these five model footings is circular; the others are the ring footings. Schematic view of the ring footing is shown in Fig. 5 and also geometric information is given in Table 1.

2.3 Test medium

In this study, uniform, clean, fine dry sand was used for the model tests. In other words, the sand soil saturation conditions are not taken into account. The particle size distribution of the sand obtained from the dry sieving method is shown in Fig. 6. This sand is classified as poorly graded sand SP in the Unified Soil Classification System (USCS). The laboratory tests were conducted on representative sand samples for gradation, specific gravity, maximum and minimum densities and strength parameters. These properties are summarized in Table 2. The friction angle of the loose sand (D_r=25%) at dry unit weight of 15.44 kN/m^3 for normal pressures of 50, 100 and 200 kPa were determined by the direct-shear testing. The measured average peak friction angle is 36° for the loose sand.

3. Experimental procedures

3.1 Preparation of the sand bed

The two sides of the tank with glass plate were marked at each 0.05m up to the base level of the model footing for preparing the sand bed. After this stage, the sand soil was carefully filled in the tank. It was performed to ensure that the model footing had full contact with the sand soil and the load applied to the footing was vertical (axial).

The sand soil with the unit weight of 15.44 kN/m^3 (i.e. the loose sand soil condition) was used in the test. To achieve the uniform density, sand soil was weighed for constant volume (0.05 m×1.0 m×1.25 m) and then carefully poured. In all tests, the minimum sand depth below the base of the model was 0.95 m.

3.2 Model tests

The model footing was placed to the predetermined location on the surface of the sand bed. The model footings were loaded using the mechanical jack supported by a reaction beam. Then, the load was measured with a calibrated stress transducer. A ball-bearing was positioned between the load cell and the model footing to ensure that no extraneous moment was applied to the model footing. The experiments were performed in the condition of stress-controlled. The constant load increment was maintained until the settlement of the model footing stabilized. The loading rate in the tests was chosen to be 3.5 mm/min. Stress distributions and settlements of the model footing were measured with the calibrated stress transducer (HTD 20149) and LVDT (Novotechnik TYP TR 50) as shown Fig. 7, respectively. One of the methods used to measure vertical stresses caused by additional loads in the soil medium is to place stress transducers in the definite depths. These transducers were also used in order to predict soil density resulting from applied loads, and in compaction theories, volume change in soil directly depends on the applied stress (Nichols *et al.* 1987, Turedi 2015). Moreover, the load-settlement and stress distribution readings were recorded by a data logger unit with sixteen-channels (MM700 Series Autonomous Data Acquisition Unit).

The tests were terminated when the failure occurred, for instance, when the load capacity of the jack was reached or when a considerable footing settlement corresponding to a

(a) LVDT

(b) Stress transducer

Fig. 7 Measuring instruments

relatively small increase in vertical load happened. After each test, the test tank was emptied and refilled for the next one to keep the conditions stable throughout the tests. Some tests were repeated twice to verify the repeatability and the consistency of the test data. The difference between two different tests with the same conditions was considered very little, and it can be neglected.

4. Numerical analyses

The numerical analysis is a powerful mathematical tool that makes it possible to solve complex engineering problems. The finite element method is a well-established numerical analysis technique used widely in many civil engineering applications, both for research and the design of real engineering problems. Different constitutive behavior of the soils can be successfully modelled with the numerical analyses. The finite element method can also be particularly useful for identifying the patterns of the deformations and stress distributions. Because of these abilities of this method, it is possible to model the construction method and to investigate the behavior of shallow footings and the surrounding soil throughout the construction process, not just at the limit equilibrium conditions (Laman and Yildiz 2007). Numerical analyses were carried out by using Plaxis 3D. It works based on a finite element package that is specially developed for the analysis of deformation and stability in geotechnical engineering problems (Plaxis 3D 2016). The stresses, strains and failure states given for any problem can be calculated. The soil and the ring footing clusters were built

Table 3 Material model parameters

Parameter	Soil	Footing
Material model	MC	LE
Drainage type	Drained	Non-porous
Unit weight, γ_n (kN/m^3)	16	77
Loading stiffness, E (kN/m^2)	9000	2×10^8
Cohesion, c (kN/m^2)	0.3	-
Poission's ratio, ν	0.2	0.3
Friction angle, ϕ (°)	36	-
Dilatancy angle, ψ (°)	6	-

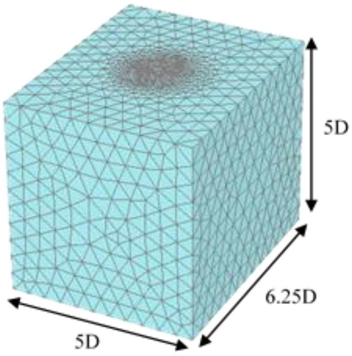

(a) Model geometry

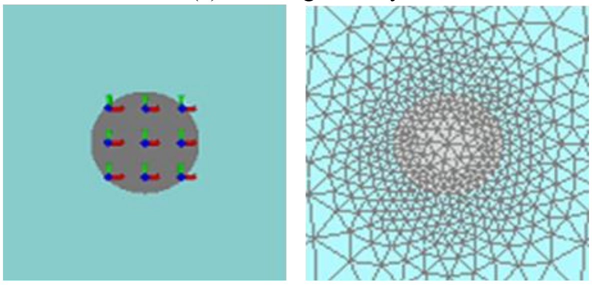

(b) r_i/R_o=0.0

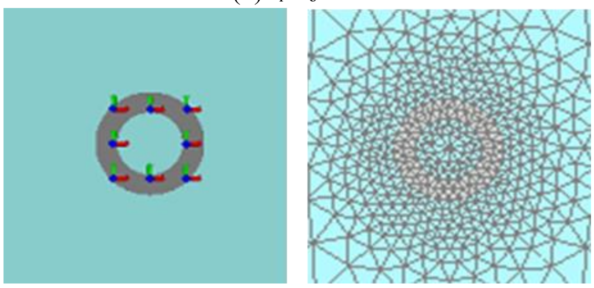

(c) r_i/R_o=0.6

Fig. 8 Geometry and finite element mesh in the numerical analyses

in with 10 nodes tetrahedral elements. Three-dimensional model is suitable for the case of the ring footing and the loading scheme on the surface area. To model the ring footing with Plaxis 3D, a working area of 5D width, 6.25D length and 5D depths was used. The finite element mesh of the problem was chosen as the medium density and it was made mesh densification in the area where the structural element was located. After dividing the finite elements, the working area consists of 16506 elements and 24325 nodes.

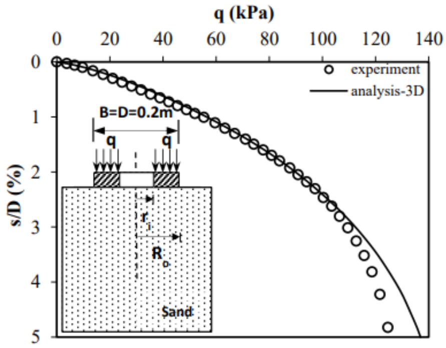

(a) r_i/R_o=0.0

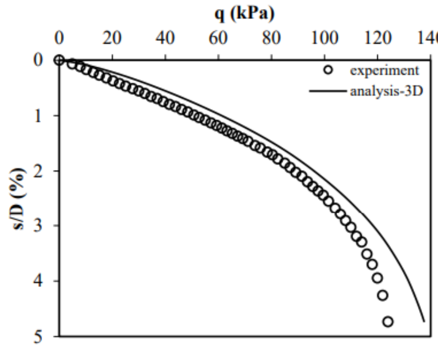

(b) r_i/R_o=0.3

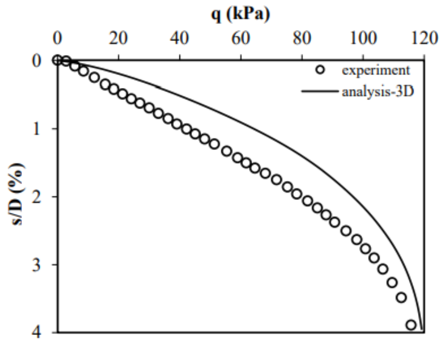

(c) r_i/R_o=0.4

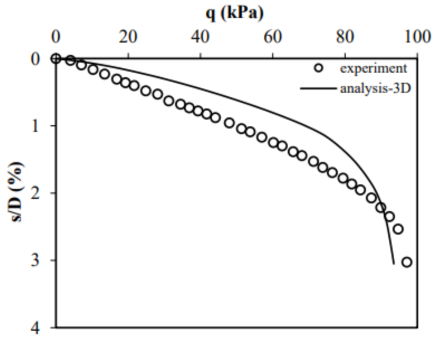

(d) r_i/R_o=0.5

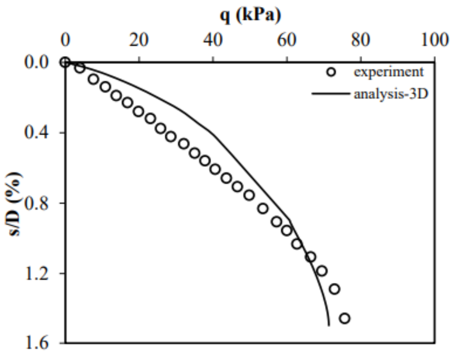

(e) r_i/R_o=0.6

Fig. 9 Load-settlement curves of the model tests with the numerical analyses

In the analyses, the bearing capacity of the footing was determined by using the plastic analysis method and the staged construction calculation method. A typical finite element mesh composed of the soil and the foundation and the geometry of the soil system used in the analyses are shown in Fig. 8. An elastic-perfectly plastic Mohr Coulomb (MC) model was chosen to stimulate the sand behavior in this study. The MC model is a practical and user-friendly model that includes only a limited number of features that the soil behavior shows in reality. The MC model involves five input parameters such as E and ν for the soil elasticity, ϕ and c for the soil plasticity and Ψ is the angle of dilatancy. The MC model represents a "first-order" approximation of the soil behavior (Plaxis 3D 2016). It is understood clearly from the literature that the sand soils are analyzed with the drained soil condition in the MC model. Table 3 shows the sand parameters used in the numerical analyses. The dilatancy angle Ψ is taken as 6°, (ϕ-30°) based on the equation proposed by Bolton (1986) and the remaining model parameters have been measured.

5. Results and discussions

5.1 Load-settlement behaviour in the model tests and the finite element analyses

A total of five model tests were conducted by using one circular footing and four different ring footings rested on the loose sand. The load-displacement curves for all kind of footing obtained from both the model tests and the finite element analyses are given in Fig. 9. The settlement ratio (s/D) is defined as the ratio of the footing settlement to the footing diameter and it is expressed by percentage. It is understood from the Fig. 9 that the load-settlement behaviors predicted by the MC model are in a good agreement with the model test results.

As clearly seen that almost the same patterns are observed. However, the values of the bearing capacities obtained from the numerical analyses are greater than those obtained from the experiments. This little difference may be due to either the soil parameters used in the analyses or the

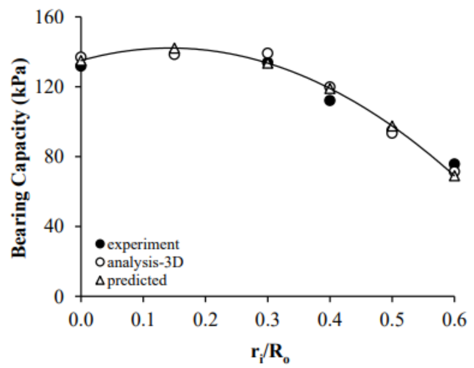

Fig. 10 Comparison of the bearing capacity results

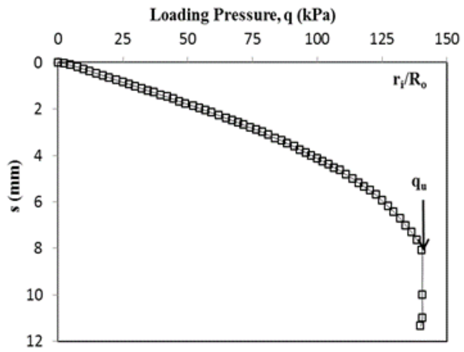

Fig. 11 General shear failure

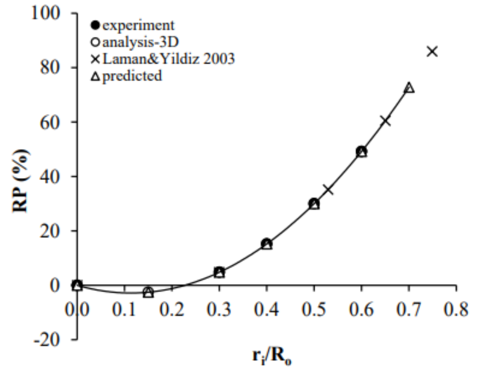

Fig. 12 RP versus r_i/R_o

values of the displacement measured in the laboratory. But in terms of the bearing capacity values, the agreement between the experimental and the numerical results is quite good as shown in Fig. 10. An equation has been recommended to calculate the bearing capacity of the ring footing in Eq. (7) with the help of experiment results. If the bearing capacity of the circular footing is known, the bearing capacity of the ring footing can be calculated by using this equation.

$$q_r = q_o - \frac{r_i}{R_o} \times \left(350 \times \frac{r_i}{R_o} - 100 \right) \tag{7}$$

5.2 Reduction percentage of bearing capacity (RP)

The type of failure in sand soil has been observed as a general shear failure. For this type of failure, a peak value of q_u is clearly defined from the curve of the load-settlement as given in Fig. 11.

The effects of the ring footing width ratio on the bearing capacity are defined in terms of the reduction percentage, RP. The term RP is used to express and compare the test data of the circular (R_o) and the ring (r_i) footing as shown in Eq. (8). The calculation of the bearing capacity decrease of the ring footings is possible with this equation.

$$RP = \frac{r_i}{R_o} \times \left(2.2 \times \frac{r_i}{R_o} - 0.5 \right) \times 100 \tag{8}$$

5.3 The effect of the ring width ratio (r_i/R_o) on RP

The value of the ultimate bearing capacity, q_u, has been calculated for each experiment. Fig. 12 shows the relation between the reduction percentage of bearing capacity (RP) with the ring width ratio (r_i/R_o) which are obtained from the experiment results, the numerical analyses and the study presented by Laman and Yildiz (2003). According to Fig. 12, the minimum RP value is reached when the ring width ratio (r_i/R_o) is 0.3 in all studies. As seen from Figs. 10 and 12, the variation in the bearing capacity is little when $r_i/R_o<0.3$. That means, when the ring width ratio, r_i/R_o, is equal to 0.3, this option can provide more economic solutions in the applications of the ring footings. Since, this corresponds to less concrete consumption in the ring footing design. Furthermore, it can be seen from the figure that a good agreement finds between the experimental and the numerical results. In the literature, some researchers found that the ring width ratio changed generally in the range of 0.2-0.4 for the ring footings (Ohri *et al.* 1997, Hataf and Razavi 2003).

5.4 Vertical stress distributions

In this section, the vertical stress distributions along the center line under the circular and the ring footings due to the applied loads are presented in Fig. 13. These distribution values obtained from the experimental and the numerical studies have been also compared with those which are calculated from the theoretical methods. The theoretical results were found by using Eqs. (1-6) presented earlier. According to Fig. 13, the similar behavior in the stress values is observed under the load (30kPa) for all footings and four different depths (z/R_o=1.25, 2.50, 3.75 and 5.00). As seen in Fig. 13, the experimental results are in a good agreement with both numerical and theoretical results. Besides, the experimental results are much closer to Boussinesq results than those of Westergaard. The experimental and numerical studies show that the stress distribution values along the center line decrease with the increase of the inner diameter of the ring footing. As expected, the vertical stress diminishes rapidly as it is reached from the soil surface to the depths. The stress value at point z/R_o=5.00 has decreased an average of 95% according to the stress value at the soil surface.

The finite element method generates an effective solution and evaluation of the displacements, stresses and forces occurring around the soil and foundation. The

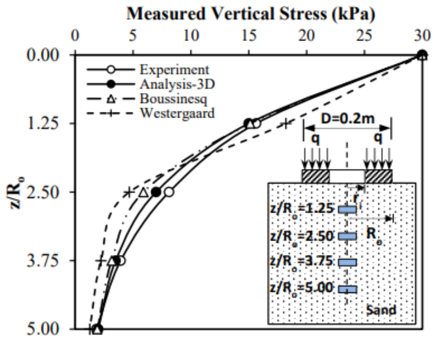

(a) r_i/R_o=0.0

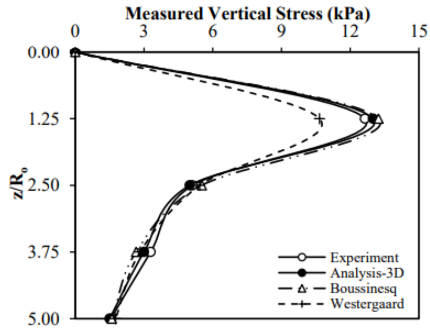

(b) r_i/R_o=0.3

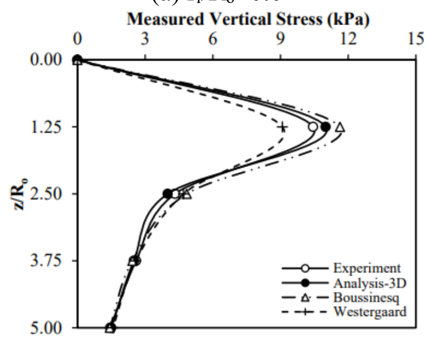

(c) r_i/R_o=0.4

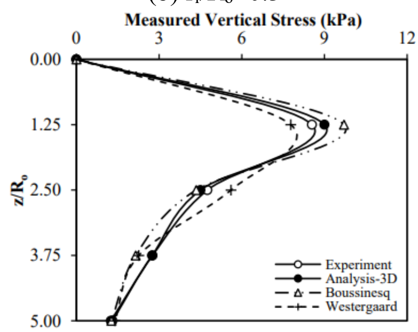

(d) r_i/R_o=0.5

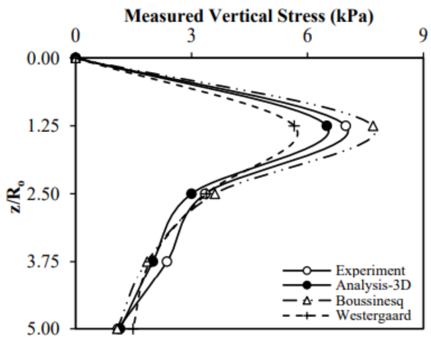

(e) r_i/R_o=0.6

Fig. 13 Vertical stress distributions

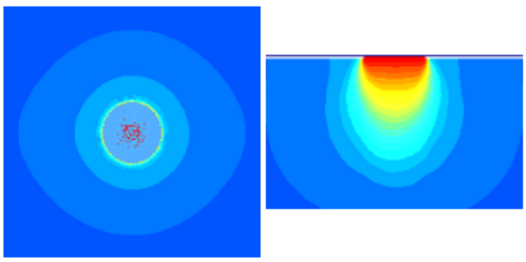

(a) r_i/R_o=0.0

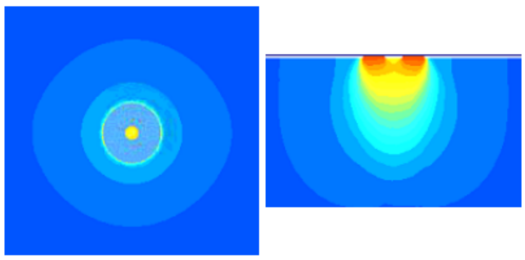

(b) r_i/R_o=0.3

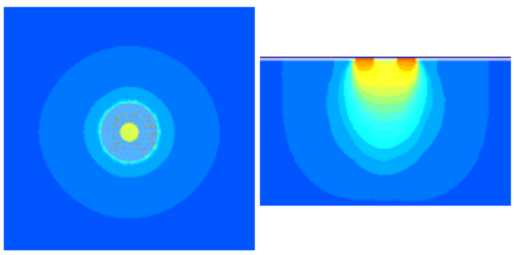

(c) r_i/R_o=0.4

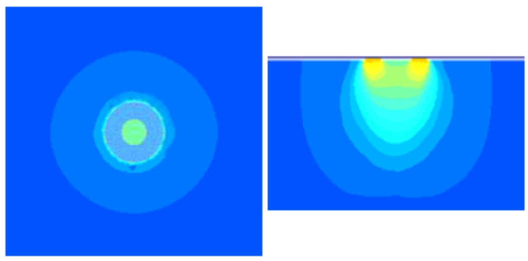

(d) r_i/R_o=0.5

Fig. 14 Vertical displacement shadings

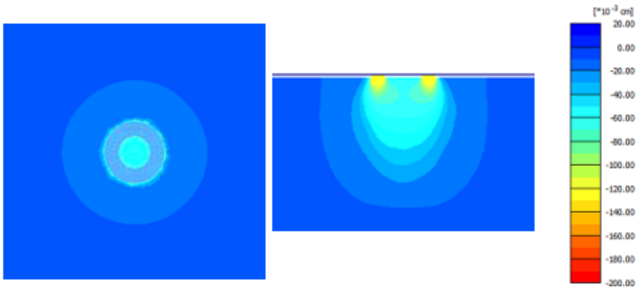

(e) r_i/R_o=0.6

Fig. 14 Continued

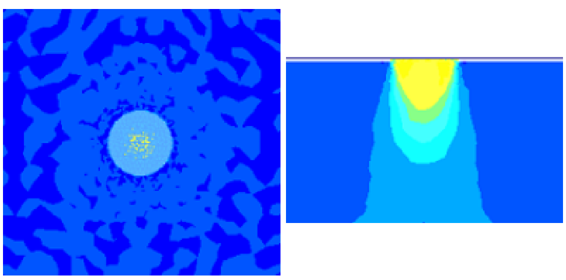

(a) r_i/R_o=0.0

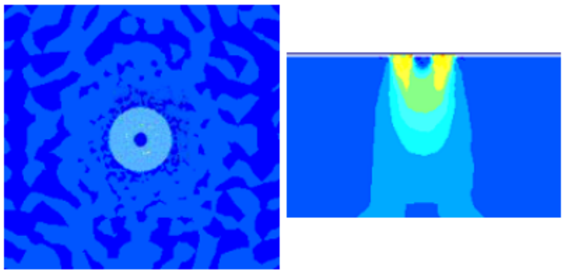

(b) r_i/R_o=0.3

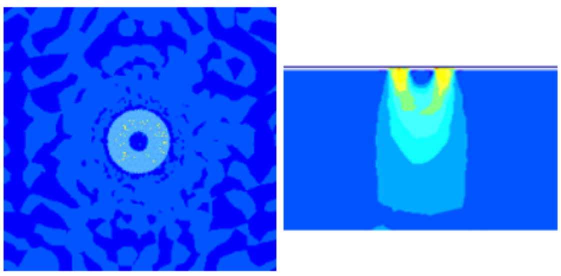

(c) r_i/R_o=0.4

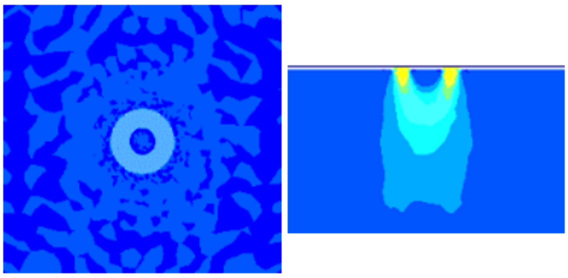

(d) r_i/R_o=0.5

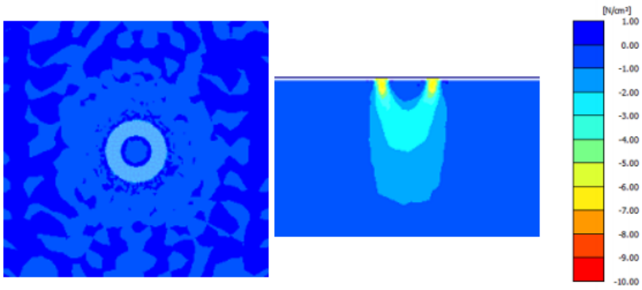

(e) r_i/R_o=0.6

Fig. 15 Vertical stress shadings

distribution of the vertical soil displacement under the footings is given Fig. 14 for all footing types which they are loaded with q=55 kPa. As shown in the figure, the displacement disturbance under the circular footing is much more than the cases with the ring footings. This means that the ring thickness causes more displacement intensification in the soil. The displacement intensification under the footing decreases with the increase of the ring width ratio (r_i/R_o). Thus, the magnitude of the displacement intensification is the highest for the circular footing (r_i/R_o=0.0). The displacement values are 2.0 mm and 1.2 mm for the circular (r_i/R_o=0.0) and the ring footings (r_i/R_o=0.6), respectively. The results obtained from the circular footing are higher approximately 65% than those obtained from the ring footing.

The distribution of the vertical stress under the footings is given in Fig. 15 for all footing types. As shown in the figure, the stress disturbance under the circular footing is much more than the cases with the ring footings. This means that the ring thickness causes more stress intensification in the soil. The stress intensification under the footing decreases with the increase of the ring width ratio. The maximum vertical stress values are 93.13 kPa and 61.14 kPa for the circular and the ring footings, respectively. The results obtained from the circular footing are higher approximately 50% than those obtained from the ring footing.

6. Conclusions

In this study, experimental and numerical investigations of the model ring footings under the ultimate load and the vertical stress distributions in the loose sand soil resulting from this are presented. The effects of the ring width on the bearing capacity of the footings and the vertical stresses along the depth are investigated. The bearing capacity-settlement curves and the vertical stress distributions obtained from the experimental and numerical studies have been given in detail. Based on the results of this investigation, the following main conclusions can be drawn:

- The bearing capacity decreases with the increase of the ring footing inner radius. The bearing capacity-settlement curves obtained from the experiments are in a good agreement with the numerical results.
- The variation in the bearing capacity is little when $r_i/R_o<0.3$, it also offers an economical solution. Moreover, this result is compatible with the literature.
- An equation is proposed to calculate the bearing capacity of the ring footings.
- The experimental results are in a good agreement with both numerical and theoretical results. Besides, these experimental results are much closer Boussinesq results than those of Westergaard.
- The magnitude of the displacement intensification is the highest for the circular footing ($r_i/R_o=0.0$). The displacement intensification under the footing decreases with the increase of r_i/R_o. The results obtained from the circular footing are higher approximately 65% than those obtained from the ring footing.
- The stress intensification under the footing decreases with the increase of r_i/R_o and the magnitude of the stress intensification is the highest for the circular footing. The results obtained from the circular footing are higher almost 50% than those obtained from the ring footing.

7. Limitations

There are some limitations to be mentioned. Firstly, it should be stated the effect of test scale. It is known that full/large-scale loading test results are valid especially for in situ conditions. However, the cost of a full-scale loading test is quite expensive for construction, instrumentation and testing. Therefore, small-scale model test facilities are used widely as an alternative to full/large-scale loading tests despite of their scale errors (Dickin and Nazir 1999). Secondly, the experiments were performed for only one soil type (i.e., sand soil condition). The results observed from this study may be different for other soils. They should also be included in future works. These additional researches are recommended as further investigations to improve the understanding the ring footing behavior comprehensively.

Acknowledgements

The second author of this study has been supported by TUBITAK (The Scientific and Technological Research Council of Turkey) with post graduate scholarship. The second author would like to express her thanks to TUBITAK for this support.

References

Anil, O., Akbas, S.O., Babagiray, S., Gel, A.C. and Durucan, C. (2017), "Experimental and finite element analyses of footings of varying shapes on sand", *Geomech. Eng.*, **12**(2), 223-238. https://doi.org/10.12989/gae.2017.12.2.223.

Azmoodeh, S. and Arafati, N. (2015), "The impact of the depth and type of soil granulation above the bearing capacity of the ring footing", *Amer. J. Civ. Eng.*, **3**(2), 75-79.

Benmebarek, S., Remadna, M.S., Benmebarek, N. and Belounar, L. (2012), "Numerical evaluation of the bearing capacity factor N'_γ of ring footings", *Comput. Geotech.*, **44**, 132-138. https://doi.org/10.1016/j.compgeo.2012.04.004.

Bhaskar, D.R.C., Shukla, S.J. and Dinesh, S. (2015), "A numerical study of foundation depth on contact stresses and settlements for various sub-soils", *Proceedings of the 50th Indian Geotechnical Conference*, Maharashtra, India, December.

Bolton, M.D. (1986), "The strength and dilatancy of sands", *Géotechnique*, **36**(1), 65-78.

Boushehrian, J.H. and Hataf, N. (2003), "Experimental and numerical investigation of the bearing capacity of model circular and ring footings on reinforced sand", *Geotext. Geomembranes*, **21**(4), 241-256. https://doi.org/10.1016/S0266-1144(03)00029-3.

Boussinesq, J.V. (1885), *Application des Potentiels à L'étude de L'équilibre et du Mouvement des Solids Elastiques*, Gauthier-Villars, France.

Choobbasti, A.J., Hesami, S., Najafi, A., Pirzadeh, S., Farrokhzad, F. and Zahmatkesh, A. (2010), "Numerical evaluation of bearing capacity and settlement of ring footing; Case study of Kazeroon cooling towers", *Int. J. Res. Rev. Appl. Sci.*, **4**(3), 263-271.

Davarci, B., Ornek, M. and Turedi, Y. (2014), "Model studies of multi-edge footings on geogrid-reinforced sand", *Eur. J. Environ. Civ. Eng.*, **18**(2), 190-205. https://doi.org/10.1080/19648189.2013.854726.

Demir, A., Yildiz, A., Laman, M. and Ornek, M. (2014), "Experimental and numerical analyses of circular footing on geogrid-reinforced granular fill underlain by soft clay", *Acta Geotechnica*, **9**(4), 711-723. https://doi.org/10.1007/s11440-013-0207-x.

Dickin, E.A. and Nazir, R. (1999), "Moment-carrying capacity of short pile foundations in cohesionless soil", *J. Geotech. Geoenviron. Eng.*, **125**(1), 1-10. https://doi.org/10.1061/(ASCE)1090-0241(1999)125:1(1).

El Sawwaf, M. and Nazir, A. (2012), "Behavior of eccentrically loaded small-scale ring footings resting on reinforced layered soil", *J. Geotech. Geoenviron. Eng.*, **138**(3), 376-384. https://doi.org/10.1061/(ASCE)GT.1943-5606.0000593.

Hanna, A. and Soliman-Saad, N. (2001), "Effect of compaction duration on the induced stress levels in a laboratory prepared sand bed", *Geotech. Test. J.*, **24**(4), 430-438. https://doi.org/10.1520/GTJ11141J.

Hataf, N. and Razavi, M.R. (2003), "Behavior of ring footing on sand", *Iran. J. Sci. Technol. Trans. B: Eng.*, **27**, 47-56.

Hazzard, J.F., Yacoub, T.E., Vijayakumar, S. and Curran, J.H. (2007), "Stresses under footings in multi-layered soils: A comparative study", *Proceedings of the 60th Canadian Geotechnical Conference*, Ottawa, Canada, October.

Kaya, N. and Ornek, M. (2013), "Experimental and numerical studies of T-shaped footings", *Acta Geotechnica Slovenica*,

10(1), 43-58.
Keshavarz, A. and Kumar, J. (2017), “Bearing capacity computation for a ring foundation using the stress characteristics method”, *Comput*. *Geotech*., **89**, 33-42. https://doi.org/10.1016/j.compgeo.2017.04.006.
Khatri, V.N., Debbarma, S.P., Dutta, R.K. and Mohanty, B. (2017), “Pressure-settlement behavior of square and rectangular skirted footings resting on sand”, *Geomech*. *Eng*., **12**(4), 689-705. https://doi.org/10.12989/gae.2017.12.4.689.
Laman, M. and Yildiz, A. (2003), “Model studies of ring foundations on geogrid-reinforced sand”, *Geosynth*. *Int*., **10**(5), 142-152. https://doi.org/10.1680/gein.2003.10.5.142.
Laman, M. and Yildiz, A. (2007), “Numerical studies of ring foundations on geogrid-reinforced sand”, *Geosynth*. *Int*., **14**(2), 52-64. https://doi.org/10.1680/gein.2007.14.2.52.
Lee, J.K., Jeong, S. and Lee, S. (2016), “Undrained bearing capacity factors for ring footings in heterogeneous soil”, *Comput*. *Geotech*., **75**, 103-111. https://doi.org/10.1016/j.compgeo.2016.01.021.
Moayed, R.Z., Rashidian, V. and Izadi, E. (2012), “Evaluation on bearing capacity of ring foundations on two-layered soil”, *World Acad*. *Sci*. *Eng*. *Technol*., **61**, 954-958.
Naderi, E. and Hataf, N. (2014), “Model testing and numerical investigation of interference effect of closely spaced ring and circular footings on reinforced sand”, *Geotext*. *Geomembranes*, **42**(3), 191-200. https://doi.org/10.1016/j.geotexmem.2013.12.010.
Nichols, T.A., Bailey, A.C., Johnson, C.E. and Grisso, R.D. (1987), “A stress state transducer for soil”, *Trans*. *ASAE*, **30**(5), 1237-1241. https://doi.org/10.13031/2013.30551.
Ohri, M.L., Purhit, D.G.M. and Dubey, M.L. (1997), “Behavior of ring footings on dune sand overlying dense sand”, *Proceedings of the 4th International Conference on Civil Engineering*, Tehran, Iran.
Ornek, M., Laman, M., Demir, A. and Yildiz, A. (2012), “Prediction of bearing capacity of circular footings on soft clay stabilized with granular soil”, *Soil*. *Found*., **52**(1), 69-80. https://doi.org/10.1016/j.sandf.2012.01.002.
Plaxis 3D (2016), *Geotechnical Finite Element Software*, Delft, The Netherlands.
Sargazi, O. and Hosseininia, E.S. (2017), “Bearing capacity of ring footings on cohesionless soil under eccentric load”, *Comput*. *Geotech*., **92**, 169-178. https://doi.org/10.1016/j.compgeo.2017.08.003.
Turedi, Y. (2015), “Stress analyses in different loading and geometry conditions”, M.Sc. Thesis, Mustafa Kemal University, Hatay, Turkey.
Turedi, Y. and Ornek, M. (2016), “Investigation of stress distributions under circular footings”, *4th International Conference on New Developments in Soil Mechanics and Geotechnical Engineering,* Nicosia, Cyprus, June.
Venkataramaiah, C. (2006), *Geotechnical Engineering*, New Age International, India.
Westergaard, H.M. (1938), *A Problem of Elasticity Suggested by a Problem in Soil Mechanics, Soft Material Reinforced by Numerous Strong Horizontal Sheets*, in *Contributions to the Nechanics of Solids*, Macmillan, U.S.A.
Yodsa-nga, P., Gasaluck, W. and Punrattanasin, P. (2012), “Stress distribution in Khon Kaen loess under spread footing”, *Elec*. *J*. *Geotech*. *Eng*., **17**, 3753-3769.

JS